Collisional angular-momentum mixing of Rydberg states of Na by He, Ne, and Ar†

T. F. Gallagher, S. A. Edelstein, and R. M. Hill
Molecular Physics Center, Stanford Research Institute, Menlo Park, California 94025
(Received 5 August 1976; revised manuscript received 24 January 1977)

The collisional angular-momentum mixing of $n = 5$–15 Na d states with the $l > 2$ states of the same n has been studied using He, Ne, and Ar as collision partners. At rare-gas pressures of ~ 1 Torr, the $l \geq 2$ states are thoroughly mixed and the mixture decays at the average radiative lifetime of all the $l \geq 2$ states of the *same* n. Using ~ 1 Torr of neon to collisionally mix the $l \geq 2$ states, the average lifetime for $l \geq 2$ was measured for each n and compared to the theoretical prediction for hydrogen, with which it is in excellent agreement. The cross section for l mixing by each of the gases is found to increase sharply from $n = 5$ to 10 and decrease above $n = 10$. The magnitudes of the l-mixing cross sections are found to correlate with the low-energy scattering lengths of the collision partners.

I. INTRODUCTION

Previously, we reported the observation of collisional angular momentum mixing of highly excited d states of Na.[1] These observations can be summarized as follows. At high pressures of Ar, He, and Ne (from 0.1 to 1 Torr), Na d states in the range $n=5$–10 were found to be mixed with the nearly degenerate higher l states of the same n (the s states, which are energetically removed from other states, did not exhibit this effect). The resulting mixture of l states radiatively decayed with the average radiative lifetime τ_{eff} of all the states of the mixture, i.e., states of the same n and $l \geq 2$. Explicitly, we have

$$\tau_{eff} = \left(\frac{1}{n^2 - 4} \sum_{l=2}^{n-1} \frac{2l+1}{\tau_l} \right)^{-1} . \quad (1)$$

τ_{eff} was observed to be independent of the rare-gas pressure over two orders of magnitude. Furthermore, when corrected for the missing s and p states, τ_{eff} was found to increase as $\sim n^{4.5}$, the predicted behavior of the average lifetime of all the l states of the same n for hydrogen.[2]

At intermediate rare-gas pressures, we observed a two-component decay, the fast component being the decay of the d state by collisions and radiation, and the slow component the decay of the mixture of $l \geq 2$ states by radiation. By measuring the fast decay rate as a function of rare-gas pressure we determined σ_l, the cross section for the collisional mixing process, and found that from $n=5$ to 10 the cross section increased proportionally to the geometrical cross section of the highly excited Na atom, i.e., as n^4. The measurements were not sufficiently accurate to tell if the cross section depended on the identity of the collision partner.

Both the intrinsic interest in the l mixing process and an improved experimental capability afforded by a more powerful N_2 laser have led us to refine and extend our initial measurements of collisional angular momentum mixing in Na. It is of interest to determine if the n^4 dependence of the cross section would continue for $n>10$. Since the valence electron of an atom in a Rydberg state is in a large loosely bound orbit and has very low kinetic energy (0.1 eV at $n=10$), it has been suggested that collision processes of atoms in Rydberg states can be related to low-energy electron scattering. For example, Fermi[3] has explained spectral shifts of alkali lines in the presence of rare gases in this way, and recently West *et al.*[4] have interpreted the collisional ionization of highly excited Xe by SF_6 using a theory of Matsuzawa,[5] which relates the ionization cross section to low-energy electron scattering. By improving our previous data, we hoped to be able to identify any correlation between collisional l mixing and low-energy electron-scattering parameters.

II. EXPERIMENTAL

The basic approach is illustrated in Fig. 1. Two dye lasers are used to successively pump Na atoms from the $3s$ state to the $3p$ state and then from $3p$ state to the nd state, and we observe the time-resolved nd-$3p$ fluorescence from the highly excited atoms. In the absence of any perturbing gas, the fluorescence decays with the d state radiative lifetime τ_d. Values for τ_{eff} are obtained by measuring the radiative decay rate at high pressures (0.1 – 1 Torr) of rare gas. The l-mixing cross sections are obtained by measuring the rate of the faster of the two exponential decay components as a function of perturbing-gas pressures.

The apparatus is shown schematically in Fig. 2. The N_2 laser is built using a transmission-line design. Typical operating parameters for the laser are: 4-nsec pulse width [full width at half-maxi-

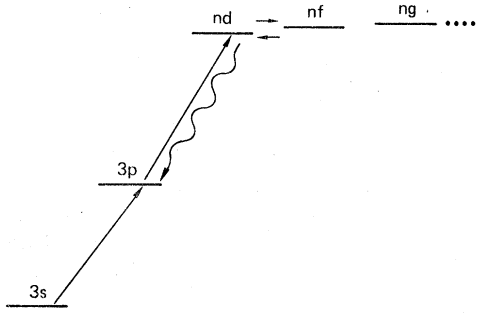

FIG. 1. Essence of the experiment for an Na nd state. Na atoms are pumped to the nd state using two photons indicated by the straight arrows. The initially populated nd state decays by radiation and collisions which populate higher l states. We observe the nd-$3p$ fluorescence to monitor the population of the nd state.

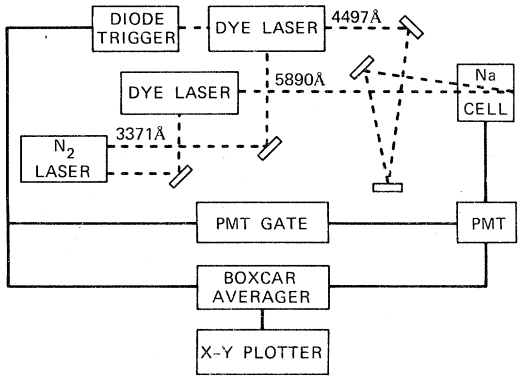

FIG. 2. Schematic diagram of the apparatus.

mum (FWHM)], 1.5-mJ pulse energy, 20-Hz repetition rate, and 15-kV charging voltage. These values are for a laser using a thyratron switch. With a spark-gap switch, the pulse energy is (25–30)% higher, but it is difficult to use a spark gap at repetition rates above 10 Hz. The dye lasers are transversely pumped lasers of the Hansch design.[6] Each laser cavity consists of a dye cell, a 20% reflecting mirror, a 20× beam expanding telescope, and a 625-lines/mm grating used in the sixth order. Typical dye-laser energies and linewidths are 40 μJ per pulse and 0.15 Å (FWHM). As indicated in Fig. 2 the path of the blue laser beam pumping the $3p$-nd transition is longer so that it reaches the cell 4 nsec after the orange laser beam pumping the $3s$-$3p$ transition to ensure that the $3p$ state is populated when the blue laser beam arrives. The two dye laser beams cross at an angle of about 1° in the cell and pass completely through the cell to a beam dump.

The cell is a Pyrex cylinder 2.2 cm in diameter, 10 cm long, which is connected to a glass vacuum system by a magnetically activated ground-glass seal. The base pressure of the vacuum system is 5×10^{-6} Torr. The temperature of the cell is monitored by a thermocouple attached to the Na reservoir (a cold finger on the cell). We operated the cell at a temperature of 150–160 °C for these measurements, which corresponds to sodium pressures of 8×10^{-6} to 2×10^{-5} Torr. The results were independent of temperature over this range. We used research-grade gases and measured the collision-gas pressures with a MKS baratron pressure gauge.

As shown in Fig. 2 we observed the fluorescence in the direction perpendicular to the laser beams. We used the appropriate Wrattan filters to block the resonance light and pass the nd-$3p$ light. For measurements of the lower states ($n\leq8$) where the decays are very fast, we used an RCA 1P28 photomultiplier tube. For $n\geq8$, we used an EMI 9558A photomultiplier which could be gated on 200 nsec after the laser pulse to eliminate scattered-light problems. We used a PAR 162 boxcar integrator for signal averaging and recorded the data on an x-y recorder. A typical trace took ~200 sec or 4000 laser pulses.

III. TWO-STATE MODEL

By analyzing the data taken in the intermediate-pressure regime, we can extract information about the collisional l-mixing rates. Since the fluorescent decays in this pressure regime are not simple one-exponential decays, we must adopt a model of the collisional l-mixing process which provides us with a functional form to which we can fit the data. Figure 3 shows the time decay of the Na 10d state in the presence of 0.027 Torr of Ne. In this inter-

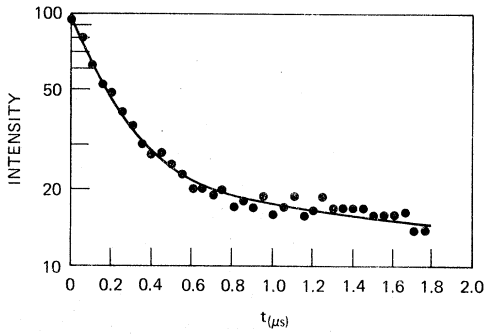

FIG. 3. Semilogarithmic plot of the initial portion of observed decay of the Na 10d state in the presence of 0.027-Torr Ne (●). This transition covers the entire fast decay but only the beginning of the slow decay. The solid line is the computer fit of two exponentials to the data. The decay times of the fast and slow component from the computer fit are 0.19 and 3.9 μsec, respectively.

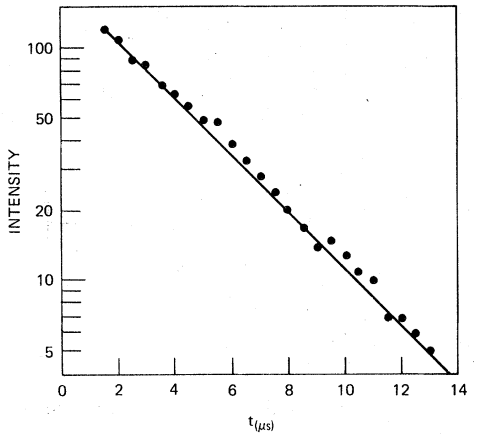

FIG. 4. Semilogarithmic plot of the later portion of the decay of the Na 10d state in the presence of 0.027-Torr Ne (●). This figure shows the slow decay, only the beginning of which is shown by Fig. 3. Treating this as a single exponential yields a decay time of 3.6 μsec.

mediate-pressure regime, a two-exponential fit, shown by the solid line, matches the data well within the statistical fluctuation of the measurement. Figure 4 shows the long-time behavior (the time scale has changed by a factor of 10) of this same decay.

We have adopted a two-state model since the data does not appear to justify a more complex approach. The two states of our model are the d state and a reservoir state r, consisting of all states for which $l \geq 3$. These two states are chosen because we initially populate only the d state with the laser and only observe fluorescence from it. We also have no direct way of monitoring population in any specific state of the $l \geq 3$ states.

Let us define A_d and A_r, the radiative rates of the d and r states, as

$$A_d = 1/\tau_d\,, \qquad A_r = \frac{1}{\tau_r} = \frac{1}{n^2-9}\sum_{l=3}^{n-1}\frac{2l+1}{\tau_l}\,, \tag{2}$$

where τ_d, τ_r, and τ_l are the radiative lifetimes of the d, r, and l states. Note that A_r is the average radiative-decay rate of states for which $l \geq 3$. Then if D and R are the populations of the d and r states, and k_r and k_d are the rates for collisions transferring atoms from the d state to the r state and vice versa, then the physical processes shown in Fig. 5 can be expressed as

$$\dot{D} = -A_d D - k_r D + k_d R, \quad \dot{R} = -A_r R - k_d R + k_r D\,. \tag{3}$$

These equations have solutions

$$D = Ae^{-k_+ t} + Be^{-k_- t}\,, \quad R = Ce^{-k_+ t} + Fe^{-k_- t}\,, \tag{4}$$

where

$$k_\pm = \tfrac{1}{2}\{K \pm [K^2 - 4(k_d A_d + k_r A_r + A_d A_r)]^{1/2}\} \tag{5}$$

and $K = k_r + k_d + A_d + A_r$. We can relate k_r and k_d by considering the high-pressure limit, where the experimentally observed single-exponential decay indicates that the l states are completely mixed, i.e., the number of atoms in each l, m_l state is equal. Then δ, the ratio of the population of the two states, is simply given by their degeneracies g_d and g_r,

$$\delta = g_d/g_r\,, \tag{6}$$

where $g_d = 5$ and $g_r = n^2 - 9$. In the high-pressure regime, a condition of quasiequilibrium exists so that

$$k_r D = k_d R\,, \tag{7}$$

and thus

$$k_d = \delta k_r\,. \tag{8}$$

The physical significance of the two decay rates k_+ and k_- can best be understood by examining the high-pressure limit, when k_r is large compared to the other rates involved. In this case K^2 is much larger than any of the terms in the parenthesis of Eq. (5) and we may use a binomial expansion to rewrite Eq. (5) as

$$k_- = (k_d A_d + k_r A_r + A_d A_r)/K \tag{9}$$

and

$$k_+ = K - (k_d A_d + k_r A_r + A_d A_r)/K\,. \tag{10}$$

From Eq. (8) it is apparent that $K = (1+\delta)k_r + A_d + A_r$. Equations (9) and (10) may be further simplified by dropping the negligible term $A_d A_r$, using the approximate value of $K \cong (1+\delta)k_r$ wherever K appears in a denominator, and again using a binomial expansion yielding

$$k_- \cong (\delta A_d + A_r)/(1+\delta) \tag{11}$$

and

$$k_+ \cong (1+\delta)k_r + A_d/(1+\delta) + \delta A_r/(1+\delta)\,. \tag{12}$$

Evaluating the right-hand side of Eq. (9) using Eqs.

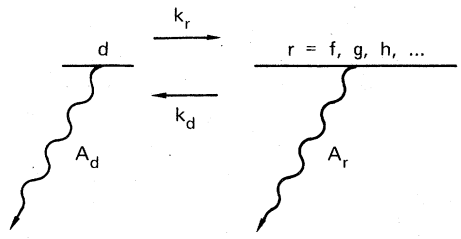

FIG. 5. Two-state model showing the radiative decay rates A_d and A_r and the collision rates k_d and k_r.

(2) and (8), we see that $k_- = 1/\tau_{eff}$, the average radiative-decay rate of the $l \geq$ states. Note that k_- is pressure independent. In the limit of high n, $\delta \to 0$ and Eq. (10) reduces to the familiar quenching relation

$$k_+ = k_r + A_d , \tag{13}$$

i.e., the fast decay rate k_+ equals the sum of the d-state radiative-decay rate and the collisional mixing rate.

σ_l is determined by fitting the pressure-dependent values of k_+ to Eq. (12). Using the relation $k_r = n\sigma_l \bar{v}$, we can write k_+ explicitly in terms of the density as follows:

$$k_+ = (1+\delta) n\bar{v}\sigma_l + A_d/(1+\delta) + \delta A_r/(1+\delta) . \tag{14}$$

Here, n is the number density of the foreign gas and $\bar{v} = (8kT/\pi\mu)^{1/2}$ is the average collision velocity, where k is the Boltzmann constant and T is the temperature in degrees Kelvin.

IV. RESULTS

We extended the previous measurements of τ_{eff} (Ref. 4) up to $n = 15$. The measurements were made by adding neon at pressures from 0.1 to 1 Torr, a high enough pressure regime to ensure complete collisional mixing of the l states. In addition, these pressures of Ne are high enough to ensure that the excited Na atoms will not diffuse out of the observation volume before decaying. Over this pressure range we observed no systematic variation in τ_{eff}. The measured values of τ_{eff} are given in Table I along with the values of τ_d showing the dramatic difference between τ_d and τ_{eff}. The values for τ_d for $n \geq 11$ are extrapolated using Eq. (2) of Ref. 8. Measurements of lifetimes for $n > 10$ gave values consistently shorter than the extrapolations of Ref. 8 (for $n = 15$ the difference was ~10%). We attribute the difference to the fact that the excited Na atoms leave the observation volume (a cylinder ~1 cm in diameter, 2 cm long) at a rate which is not insignificant compared to the radiative decay rate. In general, such effects are negligible in these experiments. The only serious limitation they impose is that it is impossible to make good measurements of the τ_{eff} (the slow decay component) at very low (<0.01 Torr) pressures of rare gas.

TABLE I. Values of Na d lifetimes τ_d, average Na lifetimes for $l \geq 2$ τ_{eff}, and extrapolated hydrogenic lifetimes τ_{av} for all l. Values for τ_{eff} were all taken using Ne as the collision partner.

n	τ_d [a] (μsec)	τ_{eff} [b] (μsec)	τ_{av} (μsec)
5	0.120(14)	0.203(12)	0.097(9)
6	0.206(24)	0.391(24)	0.209(17)
7	0.324(32)	0.796(58)	0.43(4)
8	0.502(39)	1.39(3)	0.69(10)
9	0.720(67)	2.54(17)	1.45(12)
10	0.971(35)	3.68(27)	2.21(11)
11	1.30	6.1(7)	3.60(27)
12	1.67	9.2(6)	5.4(9)
13	2.12	12.3(20)	7.5(14)
14	2.64	15.4(20)	9.7(14)
15	3.24	20.1(33)	13.0(16)

[a] $n = 5$–10 taken from Ref. 8, $n = 11$–15 extrapolated using Eq. (2) of Ref. 8.
[b] For $n = 5$–10, see Ref. 1.

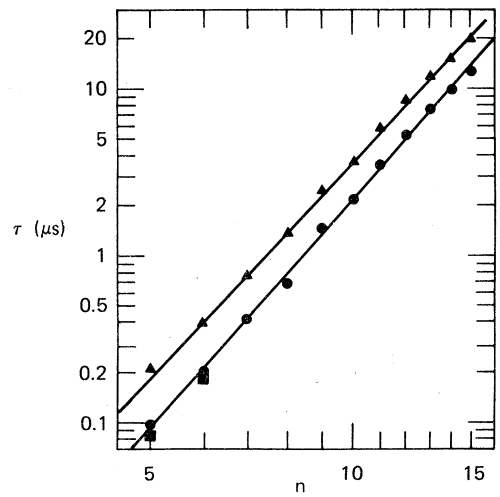

FIG. 6. Log-log plot of the observed values of τ_{eff} (▲) for the Na $l \geq 2$ states and the values of τ_{av} (●) calculated from τ_{eff}. The calculated hydrogenic values of τ_{av} (■) for $n = 5$ and 6 are also shown.

We can compare these values with the theoretical prediction for hydrogen that the average lifetime τ_{av} of all l states of the same n increases as $n^{4.5}$. We must correct for the fact that the s and p states are not collisionally mixed and that the d-state lifetimes are not the same.[2,7] Since the radiative lifetimes of hydrogen s, p, and d states all increase as n^3, as do the sodium d states, we can derive the appropriate correction from the comparison of the hydrogen s, p, and d lifetimes and the Na d lifetime for one value of n. For $n = 6$ the hydrogen s, p, and d lifetimes are 570, 41, and 126 nsec (Ref. 2) and the Na d lifetime is 206 nsec.[8] Using our measured values of τ_{eff} and correcting for the s, p, and d states, we can explicitly express a "hydrogenic" average lifetime τ_{av} for all the substates of the same n as

$$\tau_{av} = n^2 \left(\frac{n^2 - 4}{\tau_{eff}} + \frac{0.361 g_s}{\tau_d} + \frac{5.02 g_p}{\tau_d} + \frac{0.63 g_d}{\tau_d} \right) , \tag{15}$$

where g_s, g_p, and g_d are the multiplicities of the

s, p, and d states. The terms in large parenthesis represent, respectively, the statistically weighted lifetimes of the states for $l \geq 2$, the missing s state, the missing p states, and the differences in the Na and H d lifetimes. Equation (15) may be simplified to

$$\tau_{av} = n^2[(n^2-4)/\tau_{eff} + 18.6/\tau_d]^{-1} . \quad (16)$$

The values for τ_{av} generated using Eq. (14) are given in Table I and are plotted in Fig. 6 with τ_{eff}. Our values of τ_{av} increase as $n^{4.55(6)}$, in excellent agreement with the prediction for hydrogen. Furthermore, the magnitude of the observed values of τ_{av} is in excellent agreement with the $n=5$ and 6 values of τ_{av} for hydrogen 88 and 196 nsec given by Bethe and Salpeter.[4]

As indicated in Secs. I and II, the cross sections for l mixing can be determined by measuring the pressure dependence of the decay rate k_+ of the fast-decay component in the intermediate-pressure regime. Thus to determine the l-mixing collision cross sections, we focused our attention on the initial part of the decay in taking the data. We typically observed all of the fast decay but only the beginning of the slow decay. Although this procedure yields a relatively poor value for the slow decay rate k_-, it is the most accurate way of measuring k_+. The observed decays were fit by computer to two exponentials to extract values of k_+ as a function of rare-gas pressure.

In Fig. 3 we show the data for the initial fast decay of the Na 10d state and the two-exponential fit to the data. The fit gives the values of 0.19 μsec for the initial fast component (faster than the 10d-state radiative lifetime) and 3.9 μsec for the slow component, approximately equal to the $n=10$ τ_{eff} of 3.7 μsec. Since only a small part of the slow component is observed, the fit is relatively insensitive to the value of the slower decay rate (fitting the slow tail shown on the longer time scale of Fig. 4 to one exponential gives a decay time of 3.6 μsec).

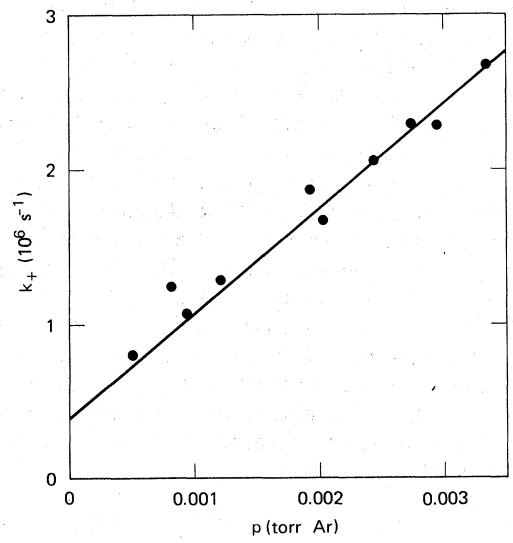

FIG. 7. Plot of k_+, the decay rate of the fast component vs argon pressure for the 14d state.

TABLE II. Cross sections for collisional l mixing of highly excited d states of Na for He, Ne, and Ar collision partners. All cross sections are in (10^3 Å^2).

n	He	Ne	Ar
5			0.29(12) [a]
6	0.38(7)	0.15(4)	0.51(20) [a]
7	0.81(10)	0.36(7)	1.50(25) [a]
8	1.05(20)	0.44(10)	2.5(10) [a]
9	1.04(20)	0.39(15)	2.4(11) [a]
10	2.2(8) [a]	0.77(12)	3.7(18) [a]
11	1.85(20)	0.60(6)	5.3(5)
12	1.69(30)	0.45(6)	5.4(7)
13	1.65(30)	0.35(4)	3.8(5)
14	1.33(20)	0.27(4)	4.0(3)
15	1.38(20)	0.27(4)	3.7(5)

[a]See Ref. 1.

No particular effort was made to make accurate measurements of the slow decay rate k_- for several reasons. First, as shown by Sec. II, the l-mixing collision rate k_r (and hence the cross section) is essentially independent of k_-. In addition, in the computer fits to the data, as shown in Fig. 3, the value of k_+ is insensitive to the value of k_-. Thus, there is really no point in making careful measurements of k_- once it has been established that the data can be fit by two decaying exponentials. Finally, it is not possible to make good measurements of k_- for high n states with Ar or He in the intermediate pressure regime (~0.002 Torr) because the excited Na atoms diffuse out of the observation region with a characteristic time comparable to τ_{eff} for $n=15$.

When the values of k_+ are plotted versus foreign gas pressure as shown in Fig. 7, the σ_l can be derived from the slope of the resulting graph using Eq. (14). The cross sections determined in this way are listed in Table II, where we have included values from Ref. 1 for completeness. σ_l for He, Ne, and Ar are presented graphically in Fig. 8. At the highest foreign gas pressures used for l-mixing studies, no effects due to quenching were observed. As shown in Fig. 8, the relative uncertainties are largest in the lower n states, where the lifetimes of the mixed state are not markedly different from the lifetime of the d state, making accurate determinations of k_+ more difficult.

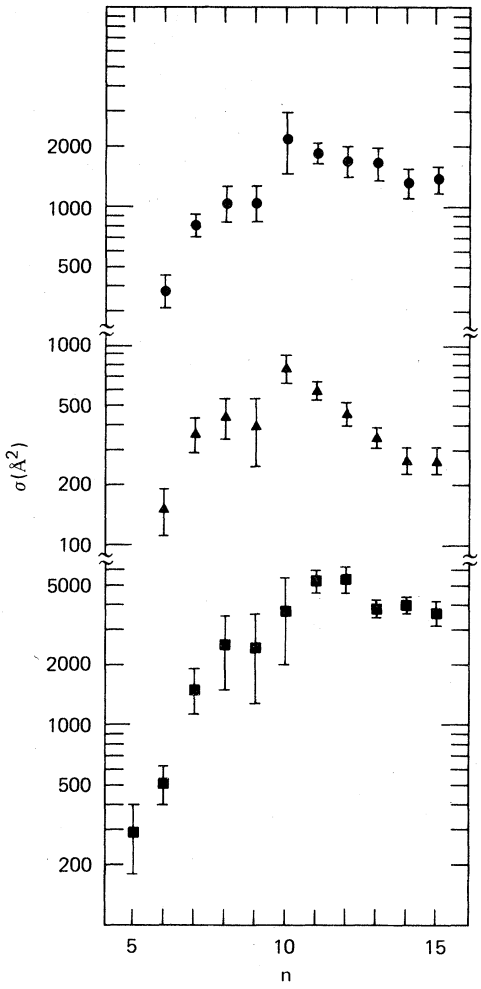

FIG. 8. Semilogarithmic plots of the He (●), Ne (▲), and Ar (■) l-mixing cross sections vs Na n state.

V. DISCUSSION

We had originally observed that the Na s states did not show collisional effects at argon pressures of up to 1 Torr and that s states thus could not be part of the collisional mixing. Since s-d and p-d energy gaps are both more than ten times as large as the d-f energy gaps, we assumed that the p states were also excluded from the collisional l mixing. This interpretation is strengthened by the excellent quantitative agreement of our values of τ_{av} (calculated assuming no collisional mixing of the p states) with the hydrogenic predictions. This gives us added confidence that in fact only the $l \geq 2$ states are collisionally mixed (at least at the rare-gas pressures we used).

The most obvious feature of our cross section observations is that the l-mixing cross sections increase rapidly as n increases from 5 to 10 but actually decrease as n increases from 10 to 15. The n dependence of the cross section can be interpreted in the following way. The l mixing is produced by the strong short-range interactions of the valence electron and the rare-gas atom. In the lower n states the probability of finding the valence electron at any point in its orbit is sufficiently high that the passage of the rare-gas atom through any part of the orbit will induce a transition from the d state to a higher l state. Consequently, the cross section for the process reflects the geometric size of the excited Na atom's orbit and increases as n^4. As n increases the volume of the excited Na atom increases as n^6, and the probability of finding the valence electron at any point decreases accordingly. From $n=10$ to 15 the electron density is sufficiently reduced that the passage of the rare-gas atom through the valence electron's orbit does not automatically induce a transition. The decreased electron density is partially offset by the increased volume with the result that the cross sections decrease slowly as n increases from $n=10$ to 15. It is in this range of n that the l-mixing cross section is most sensitive to the collision partner.

The increased precision of these measurements has shown clearly that the l mixing cross sections increase from Ne to He to Ar. The scattering lengths of Ne, He, and Ar (in atomic units) are given by O'Malley[9] to be $0.24a_0$, $1.19a_0$, and $-1.170a_0$. The fact that the l mixing cross sections increase in the same order as the magnitude of the scattering lengths leads us to view l mixing as a low-energy electron-scattering process. This view has been encouraged by the recent work of Olson.[10] He has calculated l-mixing cross sections for He, Ne, and Ar based on their scattering lengths and polarizabilities, and his calculated cross sections are in good agreement with our experimental results.

Extending and refining the previous l mixing observations have yielded significant new insights into collisional angular-momentum mixing. We hope that these insights will stimulate further theoretical and experimental interest in the problem.

ACKNOWLEDGMENTS

We would like to acknowledge many helpful discussions with R. E. Olson and W. E. Cooke and the assistance of C. Owen, Y. Walker, and M. Yokota in the laborious task of reducing the data.

†Work supported by the Air Force Office of Scientific Research under Contract No. F44620-74-C-0059.

[1]T. F. Gallagher, S. A. Edelstein, and R. M. Hill, Phys. Rev. Lett. 35, 644 (1975).
[2]H. A. Bethe and E. A. Salpeter, *Quantum Mechanics of One and Two Electron Atoms* (Academic, New York, 1957), pp. 266 and 269.
[3]E. Fermi, Nuovo Cimento 11, 157 (1934).
[4]W. P. West, G. W. Foltz, F. B. Dunning, C. J. Latimer, and R. F. Stebbings, Phys. Rev. Lett. 36, 354 (1976).
[5]M. Matsuzawa, J. Phys. B 8, 2114 (1975).
[6]T. W. Hänsch, Appl. Opt. 11, 895 (1972).
[7]P. Tsekeris and W. Happer (private communication).
[8]T. F. Gallagher, S. A. Edelstein, and R. M. Hill, Phys. Rev. A 11, 1504 (1975).
[9]T. F. O'Malley, Phys. Rev. 130, 1020 (1963).
[10]R. E. Olson, Phys. Rev. A 15, 631 (1977).